Bond graph representation of an optimal control problem for output error minimization

Omar Mouhib, Bogdan Chereji, Wilfrid Marquis-Favre, Eric Bideaux, Daniel Thomasset

Bond graph representation of an optimal control problem for output error minimization

Omar Mouhib Bogdan Chereji Wilfrid Marquis-Favre Eric Bideaux Daniel Thomasset
Laboratoire d'Automatique Industrielle
Institut National des sciences Appliquées de Lyon
25, avenue Jean Capelle
F-69621 Villeurbanne Cedex
e-mail: <firstname>.<lastname>@insa-lyon.fr

Keywords: Optimal control, output error minimization, Pontryagin Maximum Principle, port-Hamiltonian system, bicausality.

Abstract

This paper presents a new procedure based on bond graph formalism for solving an optimal control problem. The proposed procedure concerns the optimal control of linear time invariant MIMO systems where the integral performance index is based on inputs and an error between a specified output and the actual output. The proof uses the Pontryagin Maximum Principle applied to the port-Hamiltonian formulation of the system.

INTRODUCTION

The work described in this paper is a continuation of work that was started by some of the present authors and which was presented for the first time at the previous ICBGM conference in New Orleans [1]. The main idea of these research works is to introduce an optimization problem formulation into bond graph language with the perspective of coupling this to a sizing methodology of mechatronic systems. This methodology of sizing on dynamic and energy criteria using bond graph language was developed at the Laboratoire d'Automatique Industrielle [12].

Initially these research works started by giving a bond graph representation of a certain category of optimal control problem and they were restricted to linear time invariant SISO systems before they were extended to linear time invariant MIMO systems. The procedure for building the bond graph representation corresponding to the given optimal control problem has been given in[3]; it enables the set of differential-algebraic equations, that analytically gives the solution to the optimal control problem, to be supplied. In fact the obtained equations are derived graphically by assigning the bicausality to this augmented bond graph representation, skipping the analytical developments usually involved by the application of the Pontryagin Maximum Principle. A simple numerical method for solving the problem of finding the costate initial conditions from the initial set of boundary conditions has been implemented and is given in [4].

As a primary investigation, we focused on a performance index of the optimal control problem that corresponded to input and dissipative energy minimization. This is expressed as the integral of a quadratic form of the state space vector and the control input to be determined. Here we extend the procedure of the bond graph construction of an optimal control problem to another performance index, the one that corresponds to output trajectory following. Thus the performance index may be expressed as a quadratic form of error to minimize between a specified output and the actual output. The control variable is also taken into account by means of a weighting factor. Boundary conditions are supposed fixed, in particular for both final time and final state, and finally no constraint exists on either inputs or states.

The next section recalls our first proposition for the bond graph construction of an optimal control problem where the performance index corresponds to dissipative energy. Section 3 gives an extension of this proposition for the problem of following a reference trajectory, and the procedure for obtaining the corresponding augmented bond graph representation. The proof of its effectiveness is based on the Pontryagin principle applied to the port-Hamiltonian formulation of the system [5]. We show on a simple example that by applying this graphical procedure we can obtain the same result as the one that we would get by making the classical analytic developments. Finally we conclude this paper by giving some comments and perspectives for future research. Additionally, an appendix gives bases on the bicausality concept for the bond graph exploitation that gives the optimal control system.

RECALL: DISSIPATIVE ENERGY MINIMIZATION

We give in this section the principal result of the previous work concerning the bond graph construction of an optimal control problem correponding to input and dissipative energy minimization [3]:

Proposition 1: *for all optimal control problems of a linear time invariant MIMO system, with input and dissipation-based on the integral performance index of the form (1) and with given boundary conditions; we can build, from the bond graph representation of the system under study (Fig. 1), an augmented bond graph representation (Fig. 2) where its bicausal exploitation enables the system of equations that provide the optimal solution to be derived.*

$$V = \int_{t_0}^{t_f} \frac{1}{2} \left(\boldsymbol{u}_i^{\mathrm{T}} \cdot \mathbf{R}_u^{-1} \cdot \boldsymbol{u_i} + P_{\mathrm{diss}} \right) dt \tag{1}$$

where $\mathbf{R}_u$ is the control weighted matrix, $\mathbf{I}$ is the identity matrix, P_{diss} is the dissipation power expressed as the inner product of the power conjugate vectors of the R-elements ($P_{\mathrm{diss}} = \boldsymbol{e}_{\mathrm{R}}^{\mathrm{T}} \cdot \boldsymbol{f}_{\mathrm{R}}$). A multibond graph notation has been adopted [8]. In this notation GJS stands for Generalized Junction Structure.

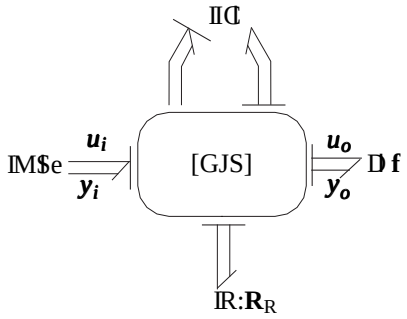

Figure 1. Model bond graph

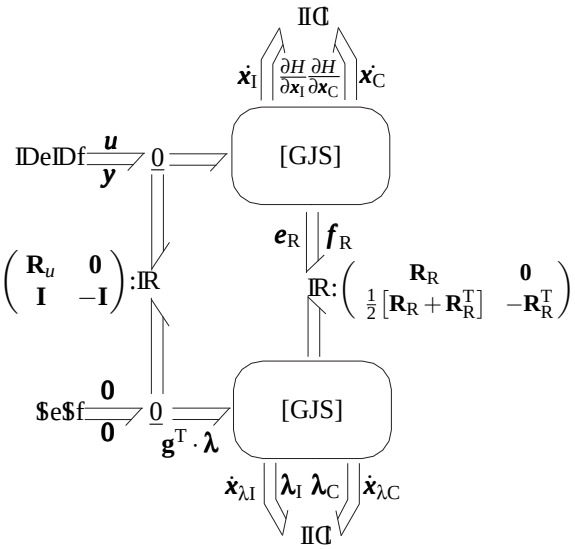

Figure 2. Generic bond graph representation of dissipative energy minimization problem

EXTENTION: PROBLEM OF FOLLOWING A REFERENCE TRAJECTORY

Knowing a trajectory defined by $\{y_r(t)\}_{t \in [t_0, t_f]}$, where t_0 and t_f indicates a horizon of fixed state, The problem is to determine the control u_i, such that for all x_0 initial states, the output error $y_o(t) - y_r(t)$ remains bounded. This problem can be formalized like a problem of quadratic error minimization on the time boundary $[t_0, t_f]$:

$$V = \min_u \int_{t_0}^{t_f} \frac{1}{2} \Big[\boldsymbol{u_i(t)}^{\mathrm{T}} \cdot \mathbf{R}_u^{-1} \cdot \boldsymbol{u_i(t)} + (\boldsymbol{y_o(t) - y_r(t)})^{\mathrm{T}} \cdot \mathbf{Q} \cdot (\boldsymbol{y_o(t) - y_r(t)}) \Big] \boldsymbol{dt} \tag{2}$$

Where Q is a weight matrix assumed diagonal, and the solution of this problem can be obtained by the following proposition:

Proposition 2: *for all optimal control problems of a linear time invariant MIMO system, with input and error-based integral performance index of the form (3) and with given boundary conditions; we can build from the bond graph representation of the system under study (Fig. 1), an augmented bond graph representation (Fig.) where its bicausal exploitation enables the system of equations that provide the optimal solution to be derived.*

The construction steps of this augmented bond graph representation of the given optimal control problem can be given according to the following procedure:

Procedure:

1. For each control to be optimally determined, add to the model bond graph an R-element characterized by the factor of the square input term in the performance index. This R-element is connected to a junction inserted onto the control source bond and corresponding to the nature of the control variable i.e. a 0 (resp. 1)-junction for an effort (resp. flow).
2. Duplicate the model bond graph with its parameters except for the R-elements. For the R-elements corresponding to the model dissipation phenomena, the characteristic matrices are transposed and their signs reversed. For the R-elements added at step 1, the characteristic matrices are the negative identity matrices. The duplicated representation is hereafter called *optimizing bond graph*.
3. For each control to be optimally determined, couple the corresponding R-elements respectively in the model and *optimizing* bond graphs by adding the identity matrix as the lower extra diagonal submatrix.
4. Replace in the optimizing bond graph the effort detectors by flow sources and the flow detectors by effort sources.

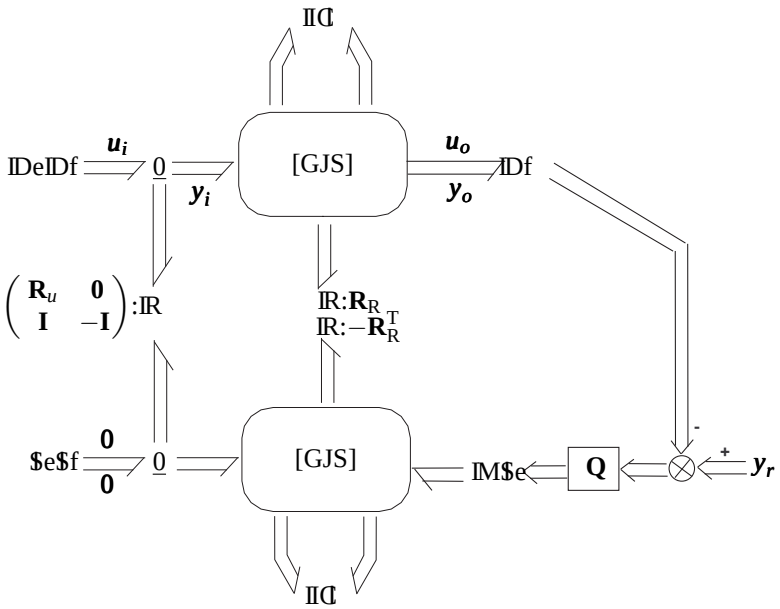

Figure 3. Generic bond graph representation of the output error minimization problem

These sources are the error between a specified output and the actual output multiplied by the coefficient **Q**.

5. Replace in the model bond graph the source elements involved in the optimal controls by double detectors and mirror them by double sources at the same place on the *optimizing bond graph*. The double sources impose both null efforts and flows.

6. Assign bicausality to the obtained bond graph. Bicausality propagates from the double sources to the double detectors and through the R-elements added at step 1. The analytical exploitation of the bicausal bond graph representation obtained provides the system equations and the optimal control solutions to the given initial problem.

DEMONSTRATION

This section proves that the bond graph representation obtained by the above procedure corresponds well to the given optimal control problem. The proof is based on the port-Hamiltonian system concept [5],[6] that has been proven to be the geometric counterpart of the graphical bond graph representation.

Port-Hamiltonian system

Consider a system with the total stored energy represented by its Hamiltonian $H(\boldsymbol{x})$ expressed in this case as a quadratic form of $\boldsymbol{x}$ (equation 3):

$$H(\boldsymbol{x}) = \frac{1}{2}\boldsymbol{x}^{\mathrm{T}} \cdot \mathbf{H} \cdot \boldsymbol{x} \tag{3}$$

where the Hessian matrix **H** is symmetric and definite positive. The port-Hamiltonian model with the hypothesis framework of a linear time-invariant system is given by (4) [6].

$$\begin{cases} \dot{\boldsymbol{x}} = [\mathbf{J} - \mathbf{S}] \cdot \frac{\partial H(\boldsymbol{x})}{\partial \boldsymbol{x}} + \mathbf{g_i} \cdot \boldsymbol{u_i} + \mathbf{g}_{\mathrm{o}} \cdot \boldsymbol{u_o} \\ \boldsymbol{y_i} = \mathbf{g}_{\mathrm{i}}^{\mathrm{T}} \cdot \frac{\partial H(\boldsymbol{x})}{\partial \boldsymbol{x}} \\ \boldsymbol{y_o} = \mathbf{g}_{\mathrm{o}}^{\mathrm{T}} \cdot \frac{\partial H(\boldsymbol{x})}{\partial \boldsymbol{x}} \end{cases} \tag{4}$$

Where **J**, $\mathbf{g_i}$ and $\mathbf{g_o}$ are constant matrices associated to junction structure transformations in the bond graph, $\mathbf{S} = \mathbf{g}_{\mathrm{R}} \cdot \mathbf{R}_{\mathrm{R}} \cdot \mathbf{g}_{\mathrm{R}}^{\mathrm{T}}$ is a constant matrix related to the dissipation phenomena where $\mathbf{g}_{\mathrm{R}}$ is a matrix associated to the junction structure transformation between the storage and the R-elements. $\boldsymbol{u}_i$ and $\boldsymbol{y}_i$ are the power conjugate variable vectors at the source ports of the system, and $\boldsymbol{u}_o$ and $\boldsymbol{y}_o$ are the power conjugate variable vectors at the detector ports of the system. The $\mathbf{g_0} \cdot u_o$ term, though it is null, is conserved to keep a trace of the equation structure and it will help to interpret some terms in what follows. A canonical bond graph representation of equation (4) is given in Fig. 1 where $\boldsymbol{x}^{\boldsymbol{T}} = \left[\boldsymbol{x}_{\mathrm{C}}^{\boldsymbol{T}}\ \boldsymbol{x}_{\mathrm{I}}^{\boldsymbol{T}}\right]$[7].

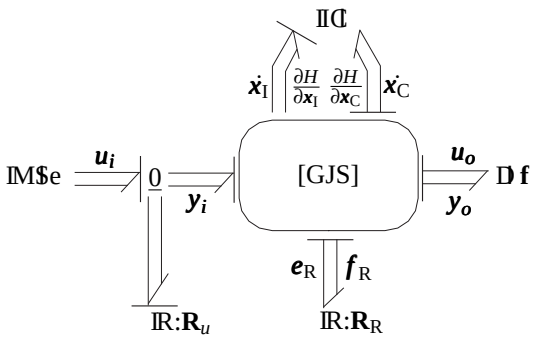

Figure 4. Canonical bond graph representation for a port-Hamiltonian system

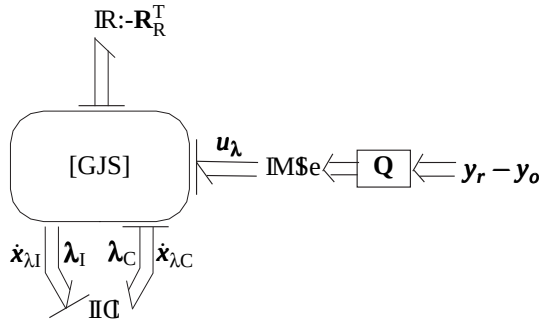

Figure 5. Bond graph translation of the equation $\dot{x}_\lambda$

Application of the Pontryagin Maximum Principle on the port-Hamiltonian system

We consider the integral performance index in the form of output error and input minimization:

$$V = \int_{t_0}^{t_f} \frac{1}{2} \left(\boldsymbol{u_i}^T \cdot \mathbf{R}_u^{-1} \cdot \boldsymbol{u_i} + (\boldsymbol{y_o} - \boldsymbol{y_r})^T \cdot \mathbf{Q} \cdot (\boldsymbol{y_o} - \boldsymbol{y_r}) \right) dt \quad (5)$$

The bond graph implementation of the control weighted matrix is displayed in Fig. 4. The Pontryagin function applied to the port-Hamiltonian system (4) with the integral performance index (5) gives:

$$\begin{aligned} H_p = \frac{1}{2} \boldsymbol{u_i}^T \cdot \mathbf{R}_u^{-1} \cdot \boldsymbol{u_i} + \frac{1}{2} (\boldsymbol{y_o} - \boldsymbol{y_r})^T \cdot \mathbf{Q} \cdot (\boldsymbol{y_o} - \boldsymbol{y_r}) \quad (6) \\ + \boldsymbol{\lambda}^T \cdot \left[[\mathbf{J} - \mathbf{S}] \cdot \mathbf{H} \cdot \boldsymbol{x} + \mathbf{g_i} \cdot \boldsymbol{u_i} + \mathbf{g_o} \cdot \boldsymbol{u_o} \right] \end{aligned}$$

where $\boldsymbol{\lambda}$ is the vector of co-state variables usually called Lagrange multipliers of the associated constrained variational problem. The set of differential-algebraic equations (7) provides the optimal solution for $\boldsymbol{x}$, $\boldsymbol{\lambda}$ and $\boldsymbol{u_i}$

$$\begin{cases} \dot{\boldsymbol{x}} = \frac{\partial H_p(\boldsymbol{x}, \boldsymbol{\lambda}, \boldsymbol{u_i})}{\partial \boldsymbol{\lambda}} \\ \dot{\boldsymbol{\lambda}} = -\frac{\partial H_p(\boldsymbol{x}, \boldsymbol{\lambda}, \boldsymbol{u_i})}{\partial \boldsymbol{x}} \\ \frac{\partial H_p(\boldsymbol{x}, \boldsymbol{\lambda}, \boldsymbol{u_i})}{\partial \boldsymbol{u_i}} = \mathbf{0} \end{cases} \quad (7)$$

We obtain:

$$\dot{\boldsymbol{x}} = [\mathbf{J} - \mathbf{S}] \cdot \mathbf{H} \cdot \boldsymbol{x} + \mathbf{g_i} \cdot \boldsymbol{u_i} + \mathbf{g_o} \cdot \boldsymbol{u_o} \quad (8)$$

$$\dot{\boldsymbol{\lambda}} = \mathbf{H} \cdot \left[\mathbf{J} + \mathbf{g_R} \cdot \mathbf{R}_R^T \cdot \mathbf{g}_R^T \right] \cdot \boldsymbol{\lambda} - \mathbf{H} \cdot \mathbf{g_o} \cdot \mathbf{Q} \cdot (\boldsymbol{y_o} - \boldsymbol{y_r}) \quad (9)$$

$$\mathbf{R}_u^{-1} \cdot \boldsymbol{u_i} + \left[\boldsymbol{\lambda}^T \cdot \mathbf{g_i} \right]^T = \mathbf{0} \quad (10)$$

While equation (8) can be derived from the Fig. 4 bond graph representation, the key issue of the bond graph formulation of an optimal control problem resides in the translation of equations (9) and (10) into this language.

Before introducing the bond graph translation of this equation, the variable mapping $\boldsymbol{x}_\lambda = \mathbf{H}^{-1} \cdot \boldsymbol{\lambda}$ is carried out. This gives :

$$\dot{\boldsymbol{x}}_\lambda = \left[\mathbf{J} + \mathbf{S}^T \right] \cdot \mathbf{H} \cdot \boldsymbol{x}_{\boldsymbol{\lambda}} + \mathbf{g_o} \cdot \boldsymbol{u_\lambda} \quad (11)$$

with $\boldsymbol{u_\lambda} = \mathbf{Q} \cdot (\boldsymbol{y_r} - \boldsymbol{y_o})$

The reason for this variable mapping is that the co-state vector $\boldsymbol{\lambda}$ is analog to co-energy variables in bond graph language while the vector $\boldsymbol{x}_\lambda$ is analog to the energy variables. It is not difficult to see that the expression (11) is closely analog to the expression of the state equations (8). In consequence Fig. 4 can be reproduced to represent the equation (11)(Fig. 5), where the power variable $\mathbf{Q} \cdot (\boldsymbol{y_r} - \boldsymbol{y_o})$ takes the same role as the one of the power variable $\boldsymbol{u_o}$.

The same development given in [3] for proving proposition 1 can be applied to treat the rest of the demonstration. Thus the equation (10), which corresponds to the Euler equation with respect to the control vector $\boldsymbol{u_i}$, can be interpreted as an effort vector balance between a vector stemming from the control vector $\boldsymbol{u_i}$ in the original system and a vector coming from the vector $\boldsymbol{\lambda}$ through the junction structure characterized by $\mathbf{g_i}$. This balance is translated by mirroring in the *optimizing bond graph* the part of the model bond graph located between the junction structure and the energy supply source (figure 6) and likewise by a concatenation of the multiport R-elements into a global multiport R-element characterized by the matrix (12).

$$\begin{pmatrix} \mathbf{R}_u & \mathbf{0} \\ \mathbf{I} & -\mathbf{I} \end{pmatrix} \quad (12)$$

Now by imposing simultaneously the null 2-flow vector balance and a null effort vector on the *optimizing bond graph* 0-junction array (figure 6), the Euler equations with respect to the $\boldsymbol{u_i}$ components (10) are verified, as the following devel-

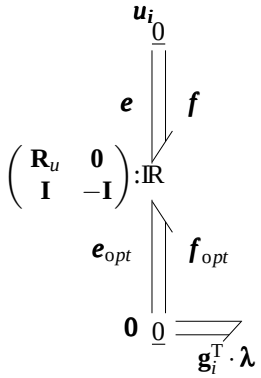

Figure 6. Bond graph translation of Euler equation with respect to $\boldsymbol{u}_i$ (10)

opment proves, using the vector notations of figure 6:

from the second vector characteristic of the R-element:
$\boldsymbol{e}_{\text{opt}} = \boldsymbol{f} - \boldsymbol{f}_{\text{opt}}$
from the null effort vector balance:
$\boldsymbol{f}_{\text{opt}} = -\mathbf{g}_i^{\text{T}} \cdot \boldsymbol{\lambda}$
from the first vector characteristic of the R-element:
$\boldsymbol{f} = \mathbf{R}_u^{-1} \cdot \boldsymbol{e} = \mathbf{R}_u^{-1} \cdot \boldsymbol{u_i}$
then:
$\mathbf{R}_u^{-1} \cdot \boldsymbol{u_i} + \mathbf{g}_i^{\text{T}} \cdot \boldsymbol{\lambda} = \mathbf{0}$

Finally the bond graph element that enables both a null effort vector and a 2-flow vector balance to be imposed on a 0-junction array is a multiport double source null effort vector and null flow vector. It is connected to the 0-junction array of the figure 6 bond graph. Such an element initializes a bicausality [10] propagation in the bond graph and thus requires the presence likewise of a multiport double detector [12],[11]. In the mathematical formulation of the optimal control design problem, the role of the control vector $\boldsymbol{u}_i$ is changed into an output vector. In this way the multiport double detector replaces the original multiport MSe element in the figure 4 bond graph. The final generic bond graph representation of the given optimal control problem is thus obtained (fig.).

EXAMPLE

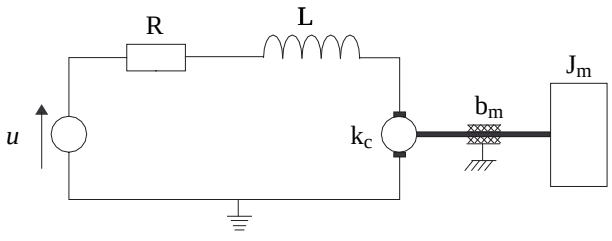

Figure 7. DC motor model

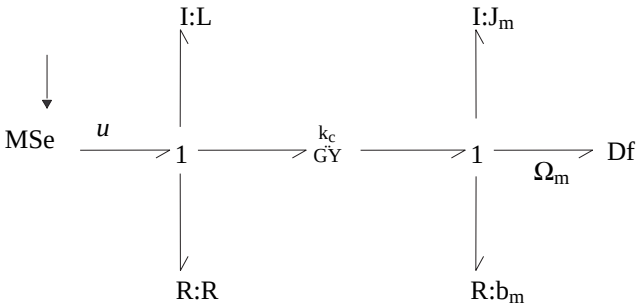

Figure 8. DC motor bond graph representation

The DC motor model is presented in Fig. 7. It consists of the armature circuit composed of a voltage source u, a resistance R and an inductance L. The electromechanical coupling is characterized by the torque constant k_c and on the mechanical side, the rotor inertia J_m and viscous friction on the rotor (parameter b_m). The model is linear and in the optimal control context, with the given initial conditions at t_0 and the final conditions at t_f, we aim at determining u which minimizes at the same time some dissipative energy and output error. Let the following integral performance index be:

$$V = \int_{t_0}^{t_f} \frac{1}{2} \left(\frac{u^2}{R_u} + P_R + (\Omega_m - \Omega_r)^2 \right) dt \qquad (13)$$

where R_u is a control weighted factor, P_R is the electrical power dissipation and $\Omega_m - \Omega_r$ is the tracking error between the actual output and the specified output.

The bond graph representation of this DC motor model is given in Fig. 8. It shows the MSe element for the voltage source, two I-elements for the two energy storage phenomena respectively associated to the magnetic energy and kinetic energies of the rotor. Two R-elements for the dissipation phenomena respectively in the electrical circuit and on the rotor. The GY-element represents the electro-mechanical coupling.

The application of both proposition 1 and proposition 2 provides the Fig. bond graph representation. The bicausality assignment as shown on the Fig. bond graph which enables the optimal control system (14) to be obtained.

$$\begin{cases} \dot{p}_1 = -\frac{R}{L} p_1 - \frac{k_c}{J_m} p_2 - \frac{R_u}{L} p_{\lambda_1} \\ \dot{p}_2 = \frac{k_c}{L} p_1 - \frac{b_m}{J_m} p_2 \\ \dot{p}_{\lambda_1} = -\frac{R}{L} p_1 + \frac{R}{L} p_{\lambda_1} - \frac{k_c}{J_m} p_{\lambda_2} \\ \dot{p}_{\lambda_2} = \frac{k_c}{L} p_{\lambda_1} + \frac{b_m}{J_m} p_{\lambda_2} + \Omega_r - \Omega_m \\ u = -\frac{R_u}{L} p_{\lambda_1} \\ y = \Omega_m = \frac{1}{J_m} p_2 \end{cases} \qquad (14)$$

The application of the Pontryagin Maximum Principle leads to the same result compared to the bond graph graphical approach for deriving the equations.

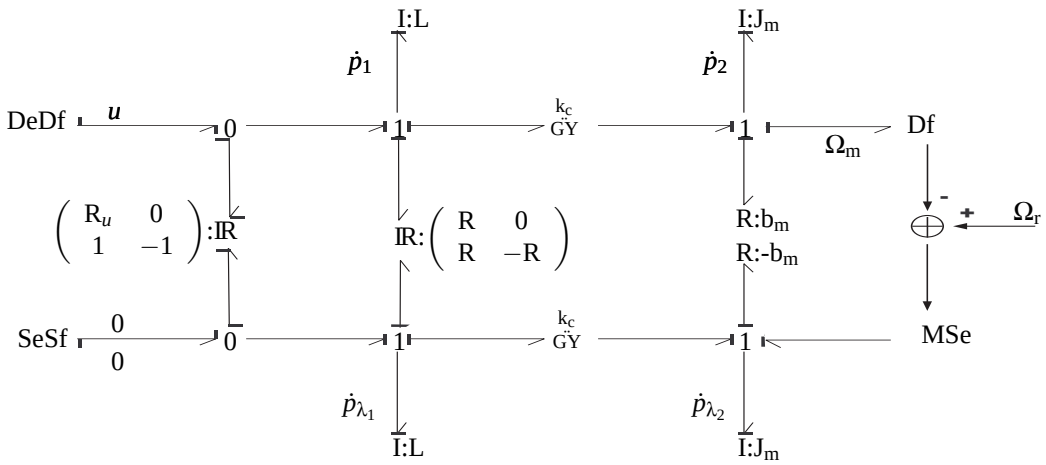

Figure 9. Bond graph representation of the DC motor optimal control problem

CONCLUSION

In this paper an extension of the originating procedure for representing the optimal control problems into bond graph with the new performance index has been given. The application of the procedure was restricted to an optimal control problem where the performance index corresponded to dissipative energy minimization. Now it has been adapted to deal with output error minimization as a performance index. Starting from the bond graph of the model, object of the optimal control problem, these procedures enable an augmented bond graph to be set up. This augmented bond graph, consisting of the original model representation coupled to an *optimizing bond graph*, furnishes, by its bicausal exploitation, the set of differential-algebraic equations that analytically give the solution to the optimal control problem. The key idea of the proof is to apply the Pontryagin Maximum Principle to a generic port-Hamiltonian system. The Port-Hamiltonian system is an analytical expression of the dynamic equations governing a model that clearly mathematically reflects the energy topology of the system model. we showed with the help of a DC motor example that we can combine both of the two procedures for solving an optimal control problem with a multiobjective in cost function, this proves the potentiality for a systematization of bond graph construction representing the optimal control formulation and the model for which the control is designed. Therefore the work still remaining is to couple these procedures to a sizing methodology based on an inverse model approach, this is one of the authors' objectives in the future.

Acknowledgement

This work has been carried out within the scope of the RNTL-METISSE project and authorised by the French Ministry of National Education and Research.

REFERENCES

[1] Marquis-Favre, W.; B. Chereji; D. Thomasset; S. Scavarda.: *Bond Graph Representation of an Optimal Control Problem: the DC Motor Example.* In: Proc. of the ICBGM'05, Int. Conf. on Bond Graph Modeling and Simulation, New-Orleans, USA, January 23-27, 2005.

[2] Fotsu-Ngwompo, R., S. Scavarda, Thomasset, D.: *Physical Model-Based Inversion in Control Systems Design Using Bond Graph Representation. Part 1 and 2: Theory and Applications.* Proceedings of the IMECHE Part I Journal of Systems and Control Engineering, vol. 215, 2001, pp. 95-112.

[3] Mouhib O., B. Chereji, W. Marquis-Favre, D. Thomasset, J. Pousin, M. Picq: *Procedure for the bond graph construction of an optimal control problem*, 26 - 28 April 2006, Paris - Cachan, France.

[4] Chereji B., O. Mouhib, W. Marquis-Favre, D. Thomasset, J. Pousin, M. Picq :*An optimal control problem: bond graph representation and solver implementation*, 5th MATHMOD, 8 - 10 February, Vienna.

[5] Maschke, B., van der Schaft, A. J.: *Port-controlled Hamiltonian systems: Modelling origins and system-theoretic properties*, in Proc. 2nd IFAC NOLCOS, Bordeaux, pp. 282-288, 1992.

[6] van der Schaft, A. J., Maschke, B.: *Hamiltonian formulation of bond graphs*, Ecole d'été d'Automatique de Grenoble, Session 22, Brogliato, B., 17-21 sept 2001.

[7] Karnopp, D.C., Margolis, D.L., Rosenberg, R.C.: *System Dynamics : Modeling and Simulation of Mechantronic Systems*. John Wiley & Sons, New York, 2000.

[8] Breedveld, P. C.: *A definition of the multibond graph language*, in "Complex and Distributed Systems: Analysis, Simulation and Control", Tzafestas, S. and Borne, P., eds., Vol. 4 of "IMACS Transactions on Scientific Computing", pp. 69-72, North-Holland Publ. Comp., Amsterdam, 1986.

[9] Gawthrop, P. J.: *Bicausal Bond Graphs.* In: Proc. of the ICBGM'95, 2nd Int. Conf. on Bond Graph Modeling and Simulation, Las Vegas, USA, January, 1995, pp. 83-88.

[10] Gawthrop, P. J.: *Physical Interpretation of Inverse Dynamics Using Bicausal Bond Graphs*. Journal of the Franklin Institute 337 (2000), pp.743-769.

[11] Fotsu-Ngwompo, R. and S. Scavarda:*Dimensioning Problems in System Design Using Bicausal Bond Graphs*. Simulation Practice and theory, vol. 7, 1999, pp. 577-587.

[12] Fotsu-Ngwompo, R., S. Scavarda, Thomasset, D.: *Physical Model-Based Inversion in Control Systems Design Using Bond Graph Representation. Part 1 and 2: Theory and Applications.* Proceedings of the IMECHE Part I Journal of Systems and Control Engineering, vol. 215, 2001, pp. 95-112.

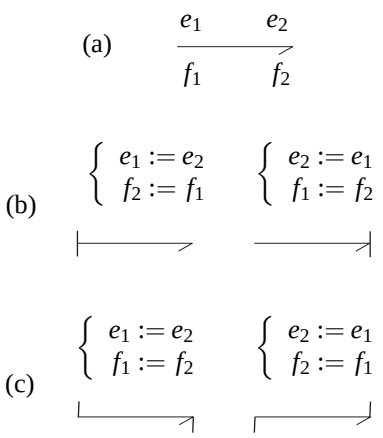

Figure 10. Power bond (a) acausal, (b) in causal assignment, and (c) in bicausal assignment

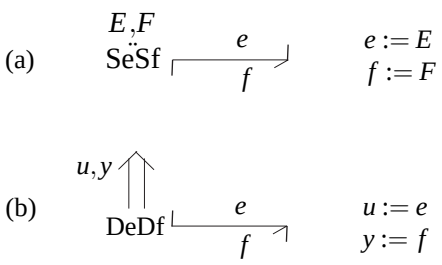

Figure 11. (a) Double source, (b) double sensor

APPENDIX: BICAUSALITY

The bicausality concept [9] is an extension of the causality concept corresponding to a strict mathematical point of view on a power bond. Considering figure 10-a acausal bond graph representation of a power bond, this can be viewed as a graphical representation of a power connection between two subsystem power ports, thus constraining the power variables (effort and flow) to be identical. The mathematical representation of this power port connection can be expressed by the two implicit equations :

$$\begin{cases} e_1 - e_2 = 0 \\ f_1 - f_2 = 0 \end{cases}$$

Causality corresponds to the organisation of these two equations with a strong physical interpretation and gives both assignment possibilities of the figure 10-b causal power bonds. However inspection of the previous implicit equations show that from a strict mathematical point of view, it is possible to have two other calculus schemes displayed in the figure 10-c so-called *bicausal* power bonds. This assignment is has no physical interpretation. It only means that both power variables are mathematically determined at the same time by the same subsystem set of equations. Interest of using bicausality, and thus this assignment, becomes obvious for deriving inverse models [10, 11, 12]. In the bicausity assignment the stroke is split in two half-strokes, one dedicated to the effort assignment (half arrow opposite side), and the other one dedicated to the flow assignment (half arrow side).

It remains now to introduce a couple of new elements in the representation that on one side initiate a bicausality assignment, and on the other side, properly terminates this bicausal assignment. The element from which bicausality starts is a double source (see Fig. 11-a) and the element where bicausality terminates is a double sensor (see Fig. 11-b).

Concerning the bond graph bicausal affectation, the element constraints are the same as for the causality assignment. The difference resides in the fact that effort and flow assignments are now uncoupled. In the bicausal bond graph, bicausality and causality coexist but jonction constraints show that two bicausal paths cannot be adjacent. Finally bicausality is assigned from one double source to a double sensor which means that these elements are present necessarly by pairs.